104 (2025) 104764

Contents lists available at ScienceDirect

Poultry Science

journal homepage: www.elsevier.com/locate/psj

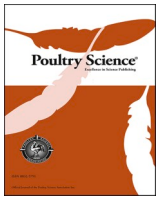

Full-Length Article

The hematopoietic function, histological characteristics, and transcriptome profiling of Wanxi white geese ovary during nesting and late-laying stages

Chunfang Zhao [a,b,c,1], Tao Jin [a,b,1], Kefeng Yang [a,b], Xinyu Liu [a,b], Man Ren [a,b], Deyong She [d], Qianqian Hu [a,b], Shenghe Li [a,b,*]

[a] College of Animal Science, Anhui Science and Technology University, Chuzhou 233100, PR China
[b] Anhui Province Key Laboratory of Animal Nutritional Regulation and Health, Chuzhou 233100, PR China
[c] Anhui Provincial Key Laboratory of Livestock and Poultry Product Safety Engineering, Hefei 236065, PR China
[d] Lu'an Academy of Agricultural Sciences, Lu'an 237008, PR China

ARTICLE INFO

Keywords:
Wanxi white geese
Nesting
Hematopoietic parameters
Serum hormone
LncRNA

ABSTRACT

Despite several factors influencing reproduction in geese, but the precise molecular mechanisms of egg cessation are not fully understood. In the present study, the hematopoietic parameters and serum hormone levels in Wanxi white geese were analyzed. RNA-Seq was utilized to identify the differentially expressed mRNAs (DEGs) and lncRNAs (DE lncRNAs) in the ovarian tissues associated with nesting in geese during the late-laying and nesting periods. Triglyceride (TG) and alkaline phosphatase (ALP) levels were higher in late-laying geese, while white blood cell (WBC), neutrophil (NEU), hemoglobin (HGB), and hematocrit (HCT) levels were significantly lower in late-laying geese. Serum levels of luteinizing hormone (LH), estrogen (E2), and progesterone (P4) increased significantly during the late-laying period, whereas prolactin (PRL) level was lower in the late-laying period than the nesting period. During the late-laying period, geese had a clear follicular hierarchy, with ovaries exhibiting mature and primary follicles. In the nesting period, the ovaries were degenerated and had many primary follicles without follicular development. Analysis of mRNA-lncRNA expression revealed 1,257 DEGs between the nesting and the late-laying stages, of which 841 were up-regulated and 416 were down-regulated DEGs. A total of 340 DE lncRNAs were identified between the nesting and the late-laying periods, with 113 being up-regulated and 227 down-regulated lncRNAs. DEGs, including *TMEM, DRD3, IGFBP7, MAPK13, GnRHR2, HECTD3, KCNU1, OPRD1,* and *VCAM1*, along with DE lncRNAs, including XR_001203613.1, XR_001206155.1, XR_001207759.1, XR_001213571.1 and XR_001214368.1 participate in reproduction in geese. Correlation analysis indicated that the cis-regulation of XR_001213096.1-*ITPR3*, XR_001203613.1-*GALNT15*, XR_001206155.1-*COL6A3*, XR_001207759.1-*ANKS1B*, and XR_001214368.1-*VPS45* participate in the molecular mechanisms underlying nesting in geese. Functional enrichment analysis revealed the DEGs and DE lncRNAs associated with focal adhesion, extracellular matrix (ECM)-receptor interaction, cell adhesion molecules (CAMs), and PI3K-Akt signaling pathways, were responsible for the differences in the ovaries between the nesting and late-laying periods. This study offers valuable information on the roles of genes and lncRNAs, and the mechanisms underlying variations in reproductive performance between the late-laying and nesting periods.

Introduction

Geese exhibit nesting behavior during the egg-laying period. Nesting shaped by natural selection, supports reproduction but impacts egg production. During the nesting period, female geese often reduce feeding and water intake, display precautionary behavior, and undergo weight loss. Furthermore, ovulation decreases significantly and laying may resume only after an extended period post-nesting (Djermanovic et al. 2024). Notably, very long nesting and significant weight loss lead to fertility loss and a reduction in egg production. Nesting is closely related to the reproductive performance of geese; thus short nesting periods can improve the reproductive performance of farmed geese,

Genetics and Molecular Biology

* Corresponding author.
E-mail address: lishhe2005@163.com (S. Li).

[1] These authors contributed equally to this work.

https://doi.org/10.1016/j.psj.2025.104764
Received 15 October 2024; Accepted 31 December 2024
Available online 1 January 2025

increasing their economic value.

Nesting in birds is primarily influenced by environmental, endocrine, and genetic factors, with genetic factors being the main factors. Nesting is regulated by reproductive hormones that interact through the hypothalamic-pituitary-ovarian axis. Bird nesting is associated with elevated levels of PRL and reduced levels of LH in the blood. Moreover, higher PRL levels and lower LH levels induce nesting behavior (Wang et al. 2021b). In poultry, LH and follicle-stimulating hormone (FSH) secretion from the anterior pituitary is regulated by hypothalamic gonadotropin-releasing hormone (GnRH). E2 induces PRL secretion, negatively impacting gonadotropin secretion. An increase in E2 secretion elevates PRL but lower LH levels (Arroba et al. 2005). Bao et al. (2023) found that the pineal gland, influenced by seasonal photoperiods, regulates the transition between the active- and non-laying periods in geese (Bao et al. 2023). Periodic melatonin secretion in response to changing photoperiods indicates that neuroendocrine factors modulate reproduction through an internal molecular response to external photoperiodic cues. Zhao et al. (2021) reported that oxidative stress and steroid biosynthesis pathways regulate reproduction seasonality in Zhedong white geese (Zhao et al. 2021).

Extensive research has been conducted on goose reproduction performance, including endocrine regulation, nutritional control, and seasonal reproduction. The characteristics of goose nesting behavior and the mechanisms underlying nesting, including endocrine factors, genetic patterns, nesting candidate genes screening, and gene polymorphisms, have been explored. Liu et al. (2022) evaluated the body size, reproductive hormones, and biochemical markers in high-yield and low-yield Wulong geese (Liu et al. 2022b). High-yield geese exhibited higher estradiol, glucose, and triglyceride levels, wider pubic spacing and abdominal circumference, shorter necks, and smaller neck and tibial circumferences than low-yielding geese. Bao et al. (2022) explored the impact of the mating behaviors of Sichuan white geese, Zhedong white geese, and Hungarian geese on their reproductive performance, primarily focusing on time preference and the frequency of successful copulations (Bao et al. 2022). The findings revealed that different geese breeds have distinct mating behaviors, and understanding these behaviors can provide key insights into enhancing the rate of successful copulation. Liu et al. (2023) bred Zhedong geese with Zi geese to reduce broodiness, resulting in significant growth heterosis and enhanced egg-laying traits in the F1 and F2 hybrids (Liu et al. 2023a). Whole genome resequencing studies have identified 7,979,421 SNPs, with three SNPs, including SNP11, in the *NUDT9* gene associated with goose broodiness. Geese reproductive traits are primarily linked with follicle growth and developmental features. Egg production depends on the quantity of undifferentiated grade follicles in the ovary. Wang et al. (2021) observed that *FAR1* and *TGFBRAP1* in geese exhibit contrasting effects on follicular granulosa cell proliferation and apoptosis. *FAR1* knockdown promotes cell proliferation and inhibits apoptosis, whereas *TGFBRAP1* knockdown enhances apoptosis (Wang et al. 2021a).

Several studies have demonstrated the crucial involvement of non-coding RNAs, including miRNAs and long non-coding RNAs (lncRNAs), in various biological processes of organisms. Ran et al. (2022) explored the gene expression profiles in geese with counter-season egg-laying and atrophic ovaries. The findings revealed the enrichment of reproductive processes, cell proliferation, and apoptosis pathways (Ran et al. 2022). Moreover, they evaluated the mechanisms regulating ovary development in non-laying geese through mRNA-miRNA analysis, offering valuable insights into the roles of miRNAs and mRNAs in reproduction. LncRNAs are RNA molecules with more than 200 nucleotides and do not code for proteins. These molecules play crucial roles in cells, such as regulating gene expression, the cell cycle, and biological signaling. LncRNAs exert their functions through various mechanisms, including transcriptional regulation, chromatin modification, RNA splicing, and transporter. Understanding lncRNA functions and mechanisms provides insights into gene regulation networks and a basis for developing practical molecular breeding approaches. Ran et al. (2021) conducted testicular histology and mRNA-lncRNA expression analysis in Landes and Sichuan white geese to explore male reproductive differences (Ran et al. 2021). Landes geese displayed a higher testicular organ index, semen volume, and seminiferous tubule diameter than Sichuan white geese. Analysis of mRNA-lncRNA revealed differential expression of spermatogenesis-related genes and significant enrichment of metabolic and phosphoinositol signaling pathways.

The Wanxi white goose is a desirable local breed that is common in the Anhui Province, China. This goose breed has several excellent traits, such as high meat quality, fast growth, strong resistance to adversity, and resistance to coarse feeding (Chen et al. 2018). In addition, it has a high yield of high-quality fluffy feathers, increasing its economic value. Consequently, this breed has become essential to the local agricultural economy. However, Wanxi white geese have a seasonal breeding pattern, with females exhibiting a high nesting rate and a low egg production rate, significantly restricting the growth of the Wanxi white geese breeding industry. The current study evaluated the hematopoietic function and histological characteristics and identified genes and lncRNAs that are differentially expressed between the nesting and late-laying stages in Wanxi white geese using transcriptome analysis. The objective of the study was to establish a comprehensive and integrated transcriptional resource that can be used for future research endeavours, providing a deeper understanding of the biological mechanisms underlying nesting. This research hypothesized that enhancing the laying performance of geese can be achieved by reducing the duration of the nesting period.

Materials and methods

Animals and experimental treatments

A total of 120 one-year-old Wanxi white geese were used in this study. The geese were from a waterfowl-breeding base at Anhui Science and Technology University, Dingyuan County, China, and were raised under the same environmental conditions and fed a commercial corn-soybean-based diet (Table 1). The protocol for using the geese was reviewed and approved by the Anhui Laboratory Animal Care Committee (experimental approval number AHSTULL2022016). All animal experimental procedures strictly adhered to the Laboratory Animal Care and Use guidelines and complied with the National Guide for Laboratory Animal Healthcare and Use standards.

Sample collection and preparation

Ten female geese were randomly selected during the nesting and late egg-laying periods. The geese were starved for 12 h before blood collection from a wing veni-puncture. The blood samples were collected

Table 1
Basal diet composition and nutrient level.

Ingredients	Content(%)	Nutrient levels	Content
Corn	49.5	Crude protein(%)	14.977
Soybean meal	20.5	Crude fat(%)	2.745
Husk powder	8.0	Metabolizable energy(MJ/kg)	10.273
Wheat bran	12.0	Energy-nitrogen ratio(%)	0.686
Lime powder	4.0	Crude fiber(%)	5.525
Premix[a]	5.0	Lys(%)	0.840
Vitamin premix[b]	0.5	Met(%)	0.270
Mildew agent	0.5		
Total	100		

[a] The premix provided the following per kg of diets: Zn 90 mg, Fe 80 mg, Mn 80 mg, Cu 20 mg, and I 0.35 mg.

[b] The vitamin premix provided the following per kg of diets: VA 9000 IU, VD_3 3000 IU, VE 24 IU, VK_3 1.8 mg, VB_{12} 0.1 mg, VB_2 5.0 mg, nicotinic acid 40 mg, pantothenate 15 mg, VB_6 3.0 mg, biotin 0.05 mg, and folic acid 0.5 mg.

in heparinized vacutainer tubes and serum vacutainer tubes. The blood in the serum vacutainer tube was centrifuged at 3000 rpm and 4 ℃ for 20 min to obtain the serum. The serum samples were stored at –80 ℃ until analysis of biochemical blood parameters. Three geese were randomly selected during the late-laying and nesting stages, and ovarian tissue samples, including hierarchical follicles, were harvested and used for histological analysis and RNA extraction.

Hematological and serum biochemical parameter analysis

The blood in the heparinized vacutainer tube was used for hematological parameter analysis. The hematological indexes were evaluated using an automatic biochemical analyzer (BC-2A103356, Shenzhen Mindray Bio-Medical Electronics Co., Ltd, Shenzhen, China). The serum samples were used to analyze blood biochemical parameters. Blood biochemical analysis was performed using an automatic serum biochemistry analyzer (ZY-310, Shanghai Kehua Bio-engineering Co., Ltd).

Serum hormone analysis

Serum samples were analyzed to determine the content of serum hormones, including PRL, LH, E2, and P4, using the relevant assay kits (Nanjing Jiancheng Bioengineering Institute, Nanjing, China). The analyses were conducted following the manufacturer's protocols. All experiments comprised three biological replicates, and statistical analysis was performed using SPSS software, version 24.0.

Histological analysis

Ovary tissues were fixed in 4 % paraformaldehyde, sliced into thin 2*3*0.5 mm sections, and soaked in tap water for 24 h. Subsequently, the samples were dehydrated using serial alcohol concentrations: 70 % overnight, 80 % for 3 h, 90 % for 2 h, 95 % I for 2 h, 95 % II for 1 h, 100 % I for 1 h, and 100 % II for 1 h. The samples were then cleared with benzyl alcohol for 20 min, xylene I for 10 min, and xylene II for 10–20 min, and then immersed in wax I for 1 h and wax II for 1 h. The samples were then embedded in paraffin wax, cut into thin 5 μm slices, stained with hematoxylin-eosin, and sealed with neutral resin before observation under a Motic B3 Microscope (Motic, Carlsbad, CA, USA).

RNA extraction and RNA sequencing

Ovarian tissue samples for RNA extraction were immediately frozen in liquid nitrogen. Total RNA was extracted using TRIzol reagent (Invitrogen, Carlsbad, CA, USA) following the manufacturer's protocol. Ribosomal RNA was eliminated to maximize coding RNA retention. The RNA was randomly fragmented and the fragments were used to synthesize the first strand of cDNA with random hexamers. The second strand cDNA was synthesized using buffer, dNTPs (with dUTP instead of dTTP), RNase H, and DNA polymerase I. The products were purified, end-repaired, and base A and sequencing junctions were added. The second cDNA strand was degraded using the UNG enzyme. Agarose gel electrophoresis was conducted to select fragment size. The final sequencing library was prepared by PCR amplification and sequenced using the Illumina HiSeqTM 4000 platform.

Quality control and transcriptome assembly

The transcriptome sequencing data were deposited in the NCBI Sequence Read Archive (SRA) database (https://www.ncbi.nlm.nih.gov/sra) under the BioProject accession numbers PRJNA1161360 and SAMN43775953 to 43775958, and the SRA project accession numbers SRR 30688733 to 30688738. The raw data were filtered to reduce analytical interference from invalid data. A quality control step was performed on the raw reads using the fastp tool to remove low-quality data and obtain clean reads. The filtering steps included removing reads containing adapter sequences, reads with more than 10 % 'N' bases, reads with all 'A' bases, and low-quality reads (with a quality value of $Q \leq 20$). The Bowtie2 tool was used to align the clean reads with the sequences in the ribosomal database. The matched ribosomal reads without mismatches were discarded, and the remaining unmapped reads were used for subsequent transcriptome analysis. After filtering, the clean reads were aligned to the reference genome (AnsCyg_PRJNA183603_v1.0) using the Hisat2 tool. Stringtie was used to assemble mapped reads for gene expression analysis after alignments with Hisat2. To identify novel transcripts, all assembled transcripts were aligned to the reference genome and classified into twelve categories using Cuffcompare. Transcripts were defined as novel ones with class codes "u," "i," "j," "x," "c," "e," or "o". Reliable novel genes were filtered based on transcript length >200 bp and ≥2 exons. These transcripts were then screened against data in Nr, KEGG, and GO databases for protein functional annotation. Gene abundance was determined using FPKM. Differential expression analysis was conducted using DESeq2 package in R software to identify differentially expressed genes between the two groups. Genes with a P-value < 0.05 and a fold-change ≥ 2 or ≤ 0.5 were considered differentially expressed.

Identification of lncRNAs

To identify lncRNAs, the transcripts were assembled using Stringtie, focusing on transcripts with more than two exons and a length exceeding 200 base pairs. Subsequently, the coding potential of the reconstructed transcripts was evaluated using CPC2 and CNCI software, with the prediction threshold set as the intersection of transcripts lacking coding ability. Differentially expressed lncRNAs were identified using DESeq2. LncRNAs with a P-value < 0.05 and a fold-change ≥ 2 or ≤ 0.5 were considered as differentially expressed.

The correlation index of between DEGs or DE lncRNAs and blood biochemical indexes was calculated using Spearman's correlation method using the OmicShare tools, a free online platform for data analysis (http://www.omicshare.com/tools).

Prediction of lncRNA target genes

Two main approaches are used in predicting genes targeted by lncRNAs: cis-target and trans-target prediction. In cis-target prediction, genes located approximately 10 kb upstream and downstream of the lncRNA are considered potential cis-target genes. In trans-target prediction, genes with a Pearson correlation coefficient above 0.95 or below –0.95 and a P-value < 0.05 relative to the lncRNA are considered trans-target genes. In antisense analysis, the RNAplex software was used to predict complementary pairing between antisense lncRNAs and mRNAs. This tool determines the optimal base pairing by calculating the minimum free energy based on the thermodynamic structure.

GO and KEGG pathway analyses

GO annotation and enrichment analysis were performed using data in the GO database (http://www.geneontology.org/). The potential biological pathways potentially regulated by the DEGs and targets of DE lncRNAs were identified using data in the Kyoto Encyclopedia of Genes and Genomes (KEGG) (http://www.genome.jp/kegg/) database. A network was constructed to illustrate the correlation between the expression of DE lncRNAs and their trans-target DEGs across samples.

Validation of DEGs and DE lncRNAs using quantitative real-time PCR

QRT-PCR analysis was used to validate the differential expression of nine genes and 12 randomly selected lncRNAs. The RNA was reverse transcribed to obtain cDNA using the RevertAid First Strand cDNA Synthesis Kit. The primers for each gene and lncRNA were generated

using the Primer Premier 5.0 tool. The primer sequences are presented in Supplementary Table S1. Real-time PCR reactions were performed using Power SYBR Green PCR Master Mix in an ABI 7500 system. Each biological replicate comprised three technical replicates. The results were presented as fold changes calculated using the $2^{-\Delta\Delta Ct}$ method. The data were expressed as mean ± standard error (SE).

Results

Blood index profiles during the nesting and late-laying periods

Hematological and serum biochemical analysis revealed that WBC, NEU, HGB, and HCT levels were significantly lower in the late-laying than in the nesting period (Table 2). Conversely, TG and ALP levels were significantly higher in the late-laying than in the nesting period (Table 3).

Serum hormone levels during the nesting and late-laying periods

The serum levels of LH, E2, and P4 were significantly higher during the late-laying than in the nesting period. Conversely, the PRL level was lower in the late-laying than in the nesting period (Fig. 1A).

Ovarian morphology during the nesting and late-laying periods

During the late-laying period, Wanxi white geese exhibited a discernible follicular hierarchy within the cortex of their ovaries, displaying a significant developmental progression. Moreover, the ovary featured mature and primary follicles during this period. Conversely, geese in the nesting period had degenerated ovaries, characterized by numerous primary follicles and arrested follicular development (Fig. 1B and C).

Global overview of mRNA and lncRNA expression profiles in the ovary

We conducted transcriptome sequencing of ovarian tissues using the Illumina HiSeq 4000 platform. After eliminating sequencing adaptors and low-quality reads from the raw data, each sample had approximately 91, 92, 95, 97, 87, and 98 million clean reads, which were utilized for subsequent analyses (Supplementary Table S2). After filtering the low-quality reads, the Q20 and Q30 values for all samples were higher than 95.58 % and 90.20 %, respectively (Supplementary Table S2). The clean reads were aligned to the geese's reference genome. The alignment results revealed that approximately 67.27 % of all mapped reads, comprising 65.64 % uniquely mapped reads and 1.63 % shared mapped reads, were captured. Approximately 55.70 % of the clean reads aligned with the exon region, 23.12 % were mapped to the intro region, and 21.18 % were mapped to the intergenic region (Fig. 2A). The proportion of gene coverage above 80 % was approximately 82 % for each group (Fig. 2B). These findings indicate high-quality RNA-Seq data; thus, it can be utilized for subsequent biological analysis.

Table 2
The differences in hematological parameters of Wanxi white geese in the nesting and late-laying periods[1].

Items	Nesting stage	Late-laying stage
WBC(10^9/L)	506.72 ± 46.62[a]	349.04 ± 20.83[b]
NEU (10^9/L)	246.79 ± 35.70[a]	54.32 ± 15.80[b]
LYM (10^9/L)	249.59 ± 58.42	290.65 ± 28.17
MON (10^9/L)	0.35 ± 0.18	0.22 ± 0.11
EOS (10^9/L)	9.34 ± 2.88	3.51 ± 0.40
BAS (10^9/L)	0.65 ± 0.13	0.34 ± 0.02
RBC(10^{12}/L)	1.78 ± 0.19	1.48 ± 0.05
HGB(g/L)	155.00 ± 8.14[a]	118.33 ± 3.18[b]
HCT(%)	31.77 ± 2.20[a]	24.57 ± 0.22[b]
MCV(fL)	180.37 ± 8.12	165.87 ± 4.43
MCH(pg)	88.80 ± 6.74	79.83 ± 3.33
MCHC(g/L)	490.67 ± 15.32	481.00 ± 9.71
RDW-CV(%)	27.40 ± 2.54	30.23 ± 1.07
RDW-SD(%)	220.83 ± 13.67	218.63 ± 12.78
PLT(10^9/L)	47.67 ± 12.45	165.00 ± 92.20
MPV(fL)	8.17 ± 0.79	7.37 ± 1.66
PDW(fL)	2.70 ± 0.00	2.30 ± 0.20
PCT(%)	0.04 ± 0.01	0.10 ± 0.04

Abbreviations: WBC, white blood cell; NEU, neutrophils; LYM, lymphocytes; MON, monocytes; EOS, eosinophils; BAS, basophils; RBC, red blood cell; HGB, hemoglobin; HCT, hematocrit; MCV, mean corpuscular volume; MCH, mean corpuscular hemoglobin; MCHC, mean corpuscular hemoglobin concentration; RDW-CV, red cell distribution width coefficient of variation; RDW-SD, red cell distribution width standard deviation; PLT, platelet count; MPV, mean platelet volume;PDW, platelet distribution width; PCT, platelet hematocrit.

[1] Data represent the means of 10 female geese.

[a-b] Means within the same rows with different superscripts are significantly different ($P < 0.05$).

Table 3
The differences in serum biochemical parameters of Wanxi white geese in the nesting and late-laying periods[1].

Items	Nesting stage	Late-laying stage
ALT(U/L)	28.00 ± 3.39	36.97 ± 1.85
ALP(U/L)	122.84 ± 9.21[b]	438.78 ± 29.44[a]
TP(g/L)	43.13 ± 6.76	38.52 ± 2.59
ALB(g/L)	16.17 ± 0.80	15.27 ± 1.00
GLOB(g/L)	26.96 ± 5.96	23.24 ± 1.64
TG(mmol/L)	0.82 ± 0.17[b]	5.93 ± 1.22 [a]
TC(mmol/L)	5.21 ± 0.78	5.71 ± 1.48
HDL(mmol/L)	2.81 ± 0.45	1.91 ± 0.57
LDL(mmol/L)	1.45 ± 0.10	2.48 ± 1.00

Abbreviations: ALT, alanine aminotransferase; ALP, alkaline phosphatase; TP, total protein; ALB, albumin; GLOB, globulin; TG, triglycerides; TC, total cholesterol;HDL, high-density lipoprotein cholesterol; LDL, low-density lipoprotein cholesterol.

[1] Data represent the means of 10 female geese.

[a-b] Means within the same rows with different superscripts are significantly different ($P < 0.05$).

Differentially expressed genes and lncRNAs between the nesting and late-laying stages

The abundance of genes was relatively consistent across all samples, with 450 novel genes identified (Supplementary Table S3), and the heatmap on the expression profiles is shown in Fig 2C. A total of 1, 257 differentially expressed genes were identified between the nesting and the late-laying period, comprising 841 up-regulated genes and 416 down-regulated genes (Fig. 2D, Supplementary Table S4). The differences in expression levels between the late-laying and nesting stages varied from 2^{-14}-fold to 2^{14}-fold. Notably, the highest fold change in gene expression between the nesting and late-laying stages was observed for ras homolog family member Q (*RHOQ*), ubiquitin-specific peptidase 36 (*USP36*), HECT domain E3 ubiquitin protein ligase 3 (*HECTD3*), and tyrosine hydroxylase (*TH*) genes. *RHOQ* and *TH* genes regulate the functioning of the endocrine system. Similarly, the abundance of lncRNAs was relatively consistent across all samples. Known lncRNAs were classified into DLEU2_5 and LINC00901 families based on Rfam analysis. Conversely, novel lncRNAs were classified into HOTAIRM1_2, SOX2OT_exon3/1, DLEU2_5, and RMST_6/8/9 families. A total of 11,886 lncRNAs were identified in this study, including 2,168 novel lncRNAs (Supplementary Table S5). Among these lncRNAs, 5 % were sense lncRNAs, 9.66 % were antisense lncRNAs, 2.29 % were intronic lncRNAs, 5.18 % were bidirectional lncRNAs, and 69.89 % were intergenic lncRNAs (Fig. 3A). LncRNAs that mapped to the reference sequence were 62.96 %, whereas the percentage of total sequenced lncRNAs was 69.70 %. Most mRNAs (73.79 %) were between 5,000 and 30,000 bp, or exceeded 50,000 bp in length. In contrast, most lncRNAs (75.38 %) ranged from 0 to 20,000 bp. Notably, compared with mRNAs

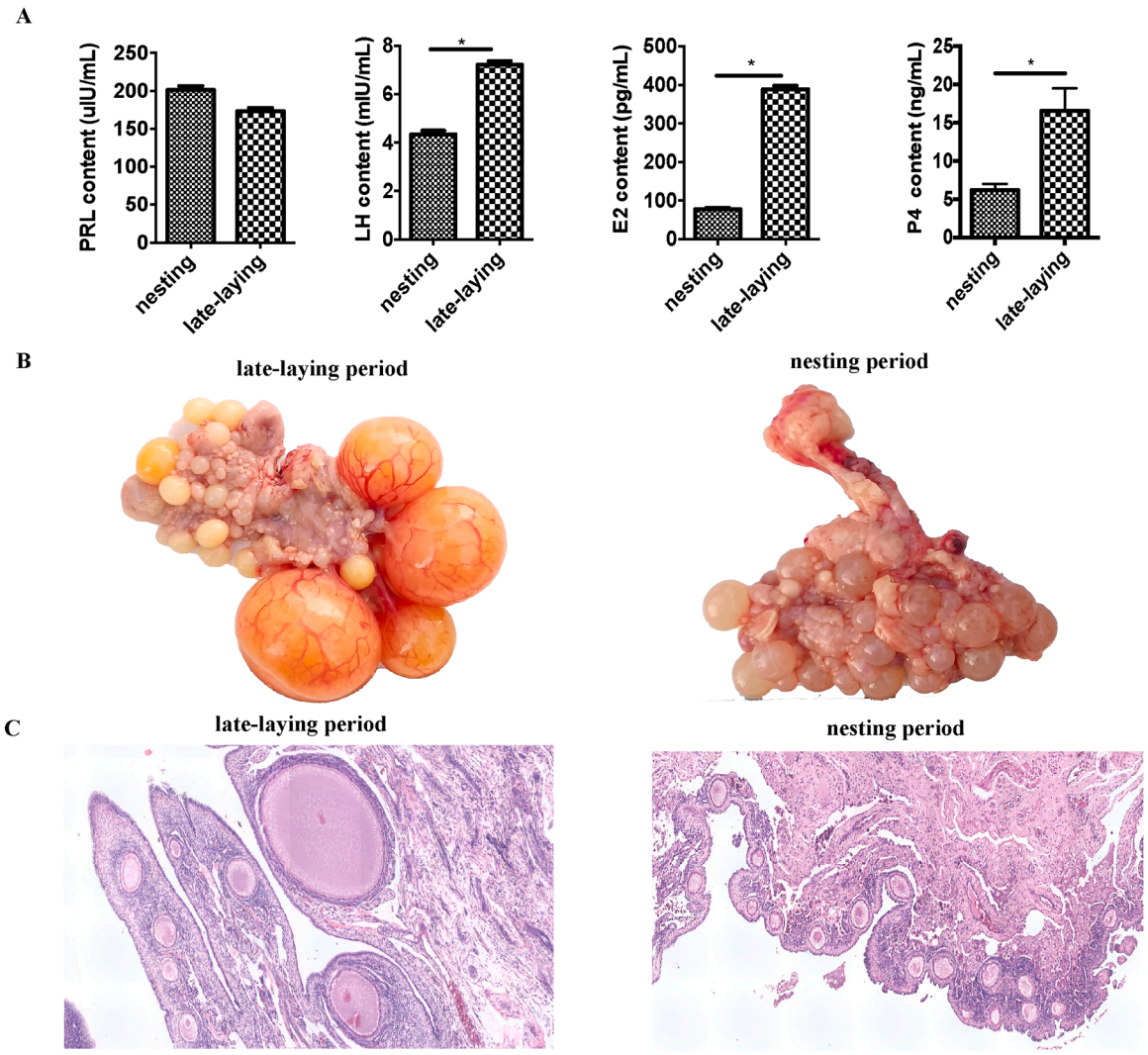

Fig. 1. Serum hormone levels and ovary histomorphometry of Wanxi white geese in the nesting and late-laying periods. A. The levels of PRL, LH, E2, and P4 in the serum in the nesting compared with late-laying period. Data represent the means of 10 female geese. *Means the values are significantly different ($P < 0.05$). B. Morphometric analysis of Wanxi white geese ovary in the nesting and late-laying periods. C. Histological analysis of Wanxi white geese ovary in the nesting and late-laying periods.

for transcripts shorter than 20,000 bp, the density of lncRNAs was significantly higher (Fig. 3B). Moreover, compared to mRNAs for transcripts containing less than five exons, the abundance of lncRNAs was markedly higher. Conversely, the density of mRNAs was significantly higher than that of lncRNAs for transcripts with more than six exons. Most lncRNAs (72.88 %) had four or fewer exons, whereas most mRNAs (76.11 %) had more than six exons (Fig. 3C). Quantitative analysis of lncRNAs and mRNAs revealed that the expression of lncRNA in the goose ovary were lower than that of mRNA transcription (Fig. 3D). In this study, 340 DE lncRNAs comprising 113 up-regulated and 227 down-regulated lncRNAs were identified (Fig. 4A, Supplementary Table S6).

Functional annotation and biological signaling pathways associated with DEGs and DE lncRNAs between nesting and late-laying periods

GO enrichment analysis was performed to explore the potential biological process, cellular component, and molecular function of the DEGs. The results showed that extracellular region, extracellular space, extracellular matrix, cell adhesion, and biological adhesion were the significantly enriched GO terms associated with the DEGs (Fig. 4B, Supplementary Table S7). In addition, the DEGs and the potential targets of the DE lncRNAs were subjected to KEGG pathway analysis. The results showed that the DEGs regulated focal adhesion, ECM-receptor interaction, cGMP - PKG signaling pathway, vascular smooth muscle contraction, neuroactive ligand-receptor interaction, CAMs, calcium signaling pathway, and PI3K-AKT signaling pathway (Fig. 4C, Supplementary Table S8).

Further analysis of the association between DE lncRNAs and mRNAs demonstrated that 143 DE lncRNAs had 190 cis-target genes, including 23 DEGs (Table 4). Additionally, 340 DE lncRNAs were associated with 5,860 trans-target genes, including 1,225 DEGs. Furthermore, 24 DE lncRNAs were associated with 22 antisense-target genes, including 5 DEGs (Figs. 5A, 6A, and 7A, Table 5). The prediction findings revealed that the DE lncRNAs target *PIGR-like* and *HBB* genes in both cis and antisense orientations. The genes are involved in the endocrine system through cis-regulation of the lncRNA XR_001213096.1-*ITPR3* and MSTRG.19948.1-*GnRHR2* and antisense-regulation of the lncRNA MSTRG.10044.1-*v-FOS*. The cis-regulation of the lncRNAs MSTRG.7055.1-*SEMA3C*, MSTRG.10806.1-*THY1*, MSTRG.18140.1-*DRD4*, MSTRG.18699.1-*OSTN*, and XR_001213096.1-*ITPR3* is involved in the functioning of the nervous system.

The potential cis-targets of DE lncRNAs were associated with bacterial-type flagellum part, microtubule bundle, SUMO ligase activity, neurotrophin TRK receptor binding, neurotrophin receptor binding, and

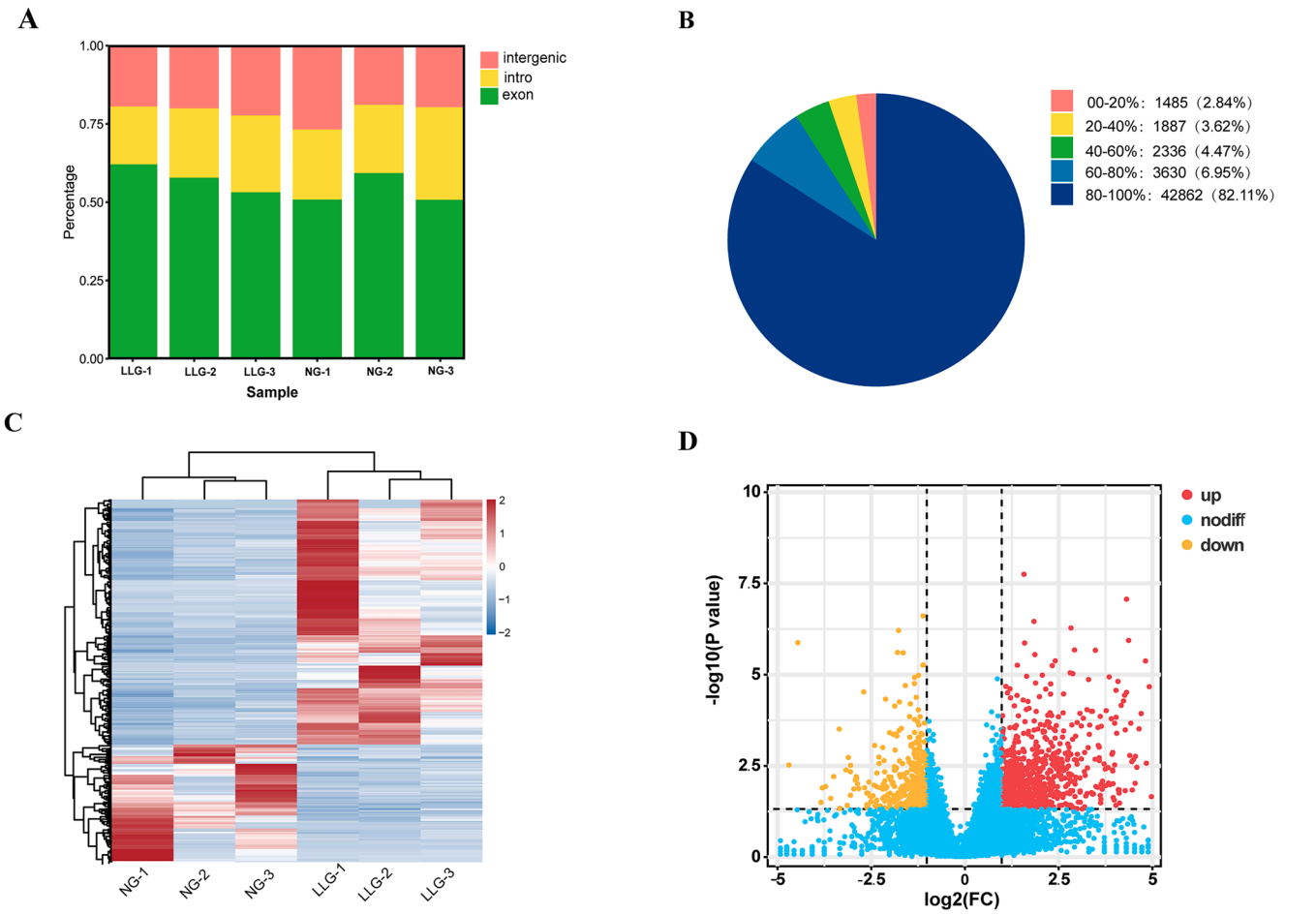

Fig. 2. Statistics for RNA sequence alignment information. A. The mapping statistics of transcriptome data. B. The proportion of gene coverage. C. The heatmap of gene expression in all samples. D. The volcano plot of DEGs in the nesting compared with late-laying periods.

MAP kinase activity (Fig. 5B, Supplementary Table S7). Moreover, these targets were enriched in the PI3K-Akt signaling pathway, dopaminergic synapse, ECM-receptor interaction, Hippo signaling pathway, and focal adhesion (Fig. 5C, Supplementary Table S8). The antisense-targets of DE lncRNAs participate in polymeric immunoglobulin receptor activity, immunoglobulin receptor activity, sublamina densa, interleukin-2 receptor binding, and receptor complex (Fig. 6B, Supplementary Table S7). Furthermore, these targets were associated with the intestinal immune network for IgA production, Th1 and Th2 cell differentiation, Th17 cell differentiation, T cell receptor signaling pathway, and cAMP signaling pathway (Fig. 6C, Supplementary Table S8).

The potential trans-targets of DE lncRNAs were implicated in the extracellular matrix, extracellular region, extracellular space, and cell adhesion (Fig. 7B, Supplementary Table S7). Moreover, these targets were associated with neuroactive ligand-receptor interaction, ribosome, leukocyte transendothelial migration, biosynthesis of amino acids, and focal adhesion (Fig. 7C, Supplementary Table S8). Network analysis revealed a strong correlation between the expression levels of 134 representative DE lncRNAs and their 37 trans-target DEGs (Supplementary Fig. S5).

Correlation analysis between blood biochemical indexes and transcriptome data

Blood biochemical index data and transcriptome data were integrated to identify key mRNAs and lncRNAs involved in regulating geese nesting. A strong correlation was identified between several genes as well as lncRNAs and key physiological parameters, including ALP, TG, WBC, NEU, HGB, HCT, PRL, LH, E2, and P4. Specific correlations were observed between the expression of certain genes or lncRNAs and the expression of one or more of the listed parameters. Several genes and lncRNAs were associated with varied physiological parameters, including *TMEM132C, DRD3, MAPK13, HECTD3*, XR_001206155.1, and XR_001213571.1 for ALP; *GnRHR2, OPRD1, RERG*, XR_001213096.1, and XR_001203613.1 for TG; *GnRHR2, HECTD3*, XR_001207759.1, and XR_001214368.1 for WBC; *KCNA5, MAPK1*3, and XR_001213571.1 for NEU; *IGFBP7*, XR_001207759.1, and XR_001214368.1 for HGB and HCT. A correlation was observed between hormonal levels (PRL, LH, E2, and P4) and the expression of specific genes, including elements such as *DRD3, GnRHR2, KCNU1, OPRD1, RERG*, XR_001203613.1, and XR_001206155.1 (Fig. 8).

Validation of gene and lncRNA expression profiles

Nine DEGs and twelve DE lncRNAs were randomly selected, and their expression patterns were assessed using qRT-PCR. The qRT-PCR results were consistent with the RNA-Seq findings. The qRT-PCR data was consistent with RNA-Seq results regarding down- or up-regulated genes and lncRNAs (Fig. 9). In summary, the validity of the RNA-Seq results was confirmed through qRT-PCR analysis using the randomly selected genes and lncRNAs.

Discussion

The reproduction period of geese breed during specific seasons varies with breeds. Female geese mainly undergo nesting, significantly

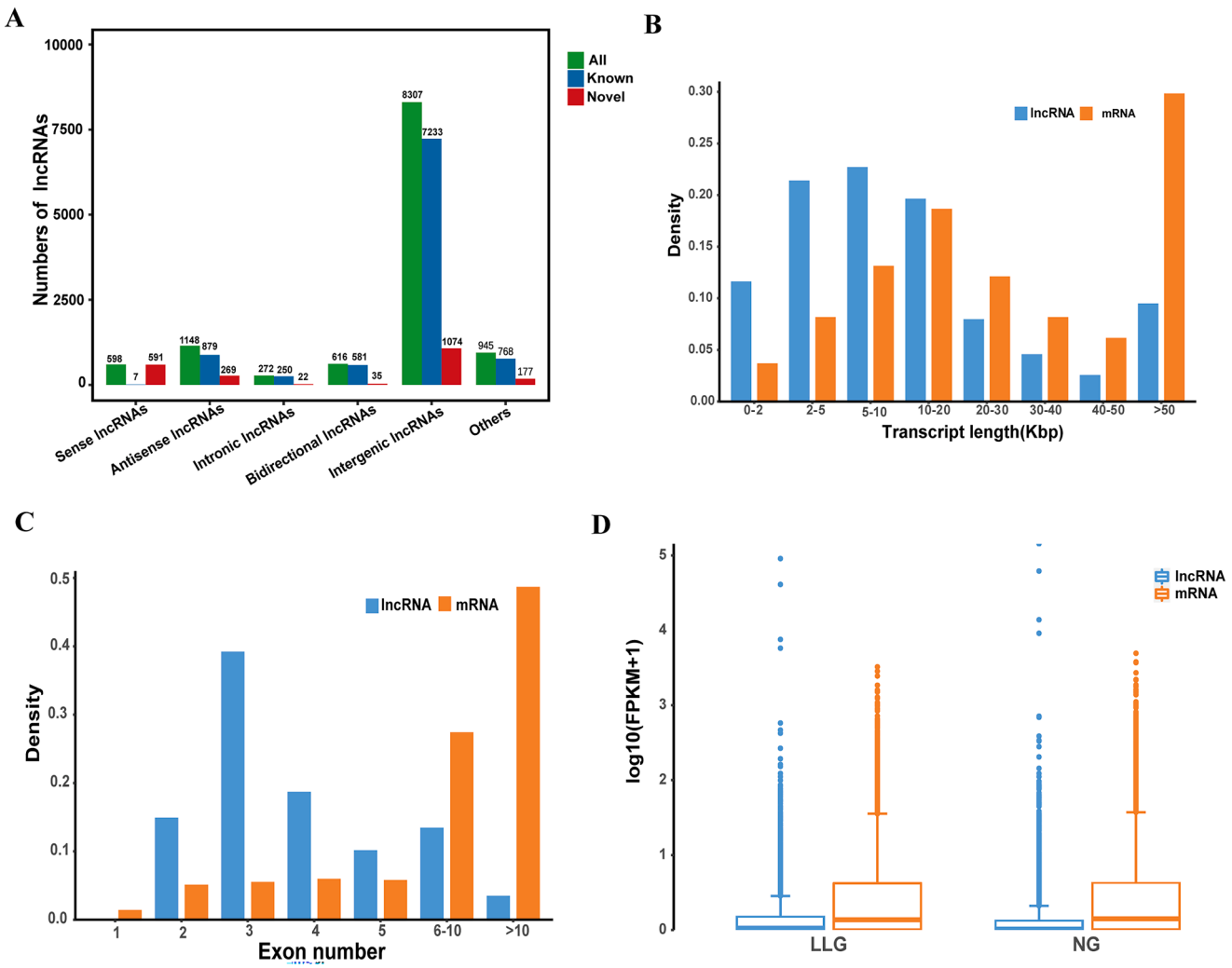

Fig. 3. The features of lncRNAs identified in the sequenced data. A. The types of lncRNAs in all samples. B. Length distribution of lncRNAs and mRNAs. C. Exon count distribution of lncRNAs and mRNAs. D. Expression profile of lncRNAs and mRNAs.

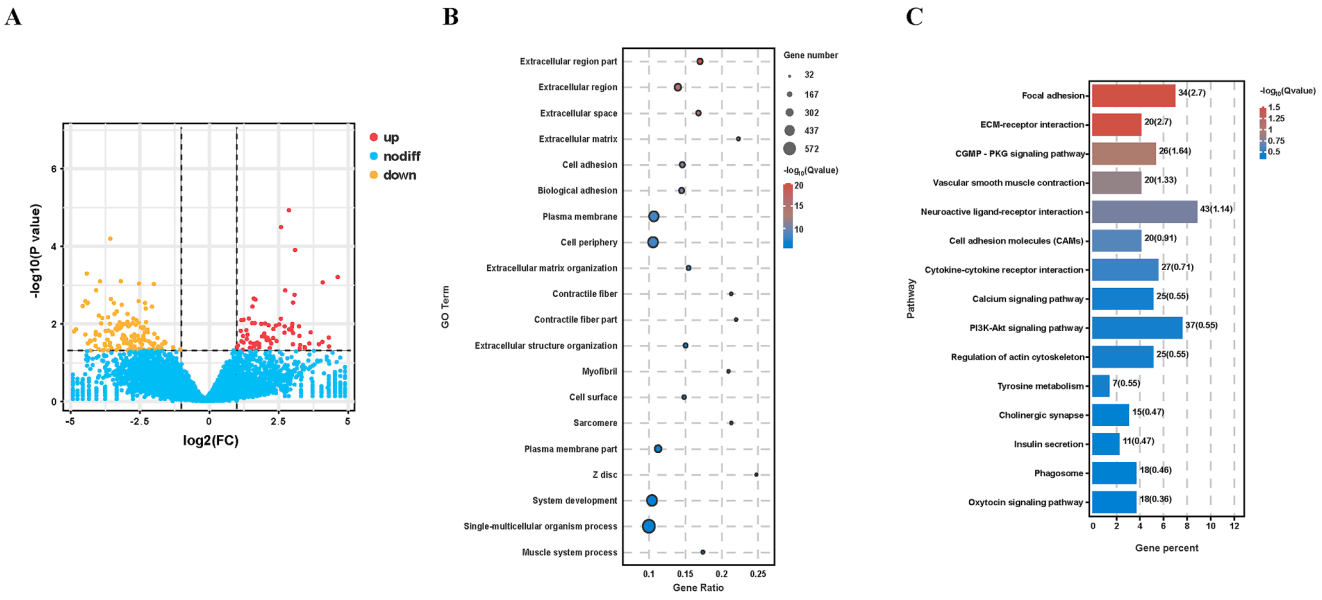

Fig. 4. GO annotation and KEGG enrichment analysis of DEGs in the nesting compared to late-laying periods. A. The volcano plot of lncRNAs in the nesting compared to late-laying periods. B. GO annotation analysis of DEGs. C. KEGG enrichment analysis of DEGs.

Table 4
The cis-target DEGs of DE lncRNAs associated with nesting in geese.

LncRNA ID	Chr	LncRNA strand	Gene strand	Up/down stream	Gene symbol	GO terms or pathway
XR_001203613.1	NW_013185661.1	-	+	upstream	*GALNT15*	O-glycan processing
XR_001204278.1	NW_013185666.1	-	+	upstream	*CORO1C*	regulation of protein phosphorylation
MSTRG.4681.1	NW_013185674.1	-	-	upstream	*OIH*	protein binding
XR_001206155.1	NW_013185684.1	+	-	downstream	*COL6A3*	ECM-receptor interaction
XR_001206156.1	NW_013185684.1	+	-	downstream	*COL6A3*	ECM-receptor interaction
XR_001206230.1	NW_013185685.1	+	+	upstream	*CHAD*	ECM-receptor interaction
MSTRG.7055.1	NW_013185693.1	-	-	downstream	*SEMA3C*	signal transduction
XR_001207759.1	NW_013185706.1	-	-	upstream	*ANKS1B*	receptor localization to synapse
MSTRG.10806.1	NW_013185736.1	+	+	upstream	*THY1*	regulation of protein phosphorylation
MSTRG.12265.1	NW_013185757.1	-	+	downstream	*PIGR-like*	cell communication
XR_001213096.1	NW_013185867.1	+	+	upstream	*ITPR3*	oxytocin signaling pathway, estrogen signaling pathway
XR_001213174.1	NW_013185872.1	-	-	downstream	*KCNA5*	regulation of hormone levels
XR_001213571.1	NW_013185898.1	+	+	downstream	*RERG*	cell communication
MSTRG.18140.1	NW_013185898.1	+	+	upstream	*DRD4*	neuroactive ligand-receptor interaction, dopaminergic synapse
MSTRG.18699.1	NW_013185920.1	-	-	upstream	*OSTN*	hormone activity
MSTRG.19835.1	NW_013185966.1	+	-	downstream	*HBB*	transport
MSTRG.19948.1	NW_013185972.1	+	+	downstream	*GnRHR2*	GnRH signaling pathway, neuroactive ligand-receptor interaction
MSTRG.19948.1	NW_013185972.1	+	-	upstream	*ANKRD34C*	carbohydrate metabolic process
XR_001214368.1	NW_013186002.1	-	+	downstream	*VPS45*	synaptic signaling
MSTRG.20799.2	NW_013186024.1	-	-	downstream	*FBXO40*	protein polyubiquitination
MSTRG.21222.2	NW_013186063.1	+	-	downstream	*COL6A2*	ECM-receptor interaction
XR_001204878.1	NW_013185654.1	-	-	downstream	*SFTPA1*	–
MSTRG.1307.1	NW_013185657.1	+	-	upstream	*ASTL*	–

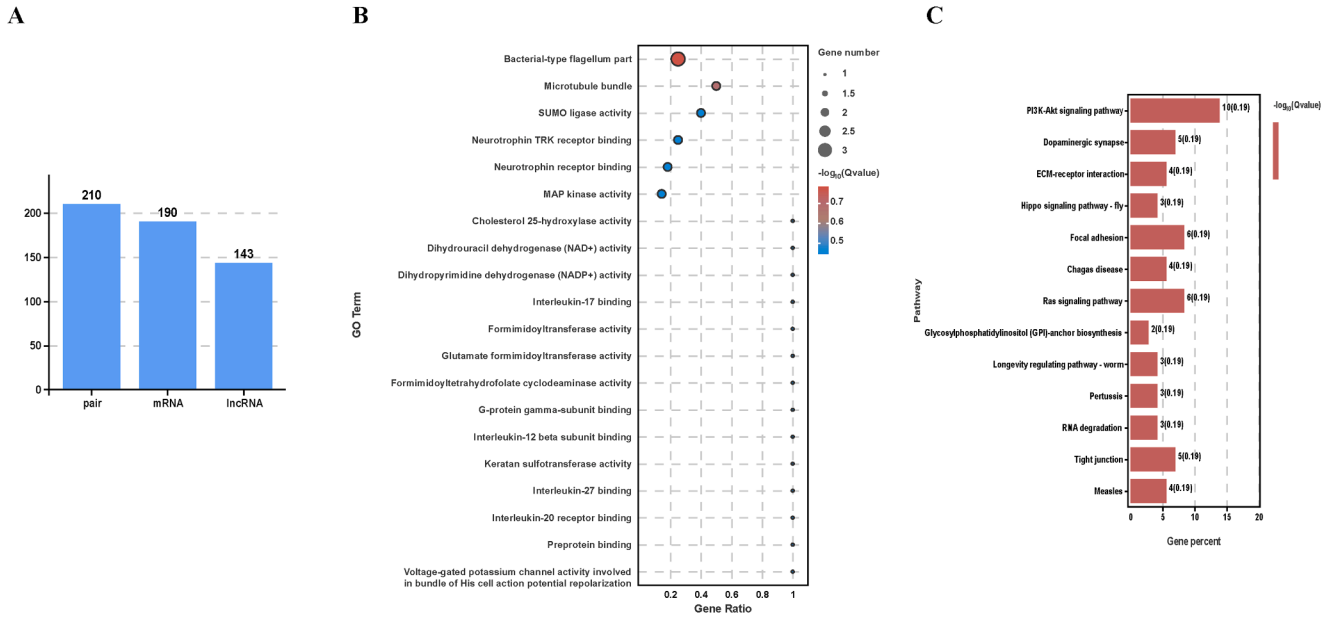

Fig. 5. GO annotation and KEGG enrichment analysis of cis-targets of DE lncRNAs in the nesting compared to late-laying periods. A. Histogram of the number of lncRNA-mRNA cis-target gene pairs and the corresponding number of lncRNAs and mRNAs. B. GO annotation analysis of cis-targets of DE lncRNAs. C. KEGG enrichment analysis of cis-targets of DE lncRNAs.

reducing the number of eggs laid annually (Djermanovic et al. 2024). During the nesting period, geese enhance their immune system by improving the production of WBC, with a significant increase in NEU. Follicle formation is prioritized during the laying period, reducing the burden on the immune system. In this study, the nesting geese exhibited a significant increase in WBC, NEU, HGB, and HCT levels. During the egg-laying phase, estrogen stimulates the liver to produce lipids, especially TG, creating an energy reserve for the embryo (Alvarenga et al. 2011). Palo et al. (1995) observed that broilers exhibited the highest ALP activity at two weeks old, coinciding with the absorption of the yolk sac and the development of locomotory independence (Palo et al. 1995). Egg-laying birds exhibit a temporary increase in ALP activity. In the current study, TG and ALP levels were significantly higher in the late-laying geese, consistent with previous reports. E2 and LH levels fluctuate over the breeding cycle. High E2 levels promote egg production and egg formation. Conversely, PRL plays a pivotal role in sustaining nesting behavior, and the peak of LH production occurs at the onset of the egg-laying period (Soriano et al. 2018). In this study, the serum levels of LH, E2, and P4 were significantly elevated, whereas the PRL level was lower during the late-laying period.

Transcriptome profiling results showed the highest fold change in the expression of *USP36, HECTD3,* and *TH* genes during the nesting period relative to the late laying period. RNA helicase DHX33, a critical regulator of rRNA synthesis and mRNA translation during embryonic development, is destabilized by the loss of *USP36*, a deubiquitinating enzyme, significantly affecting embryo viability (Fraile et al. 2018). Furthermore, compared with normal ovaries, *USP36* is overexpressed in ovarian cancer cells and tissues, highlighting its potential role as a

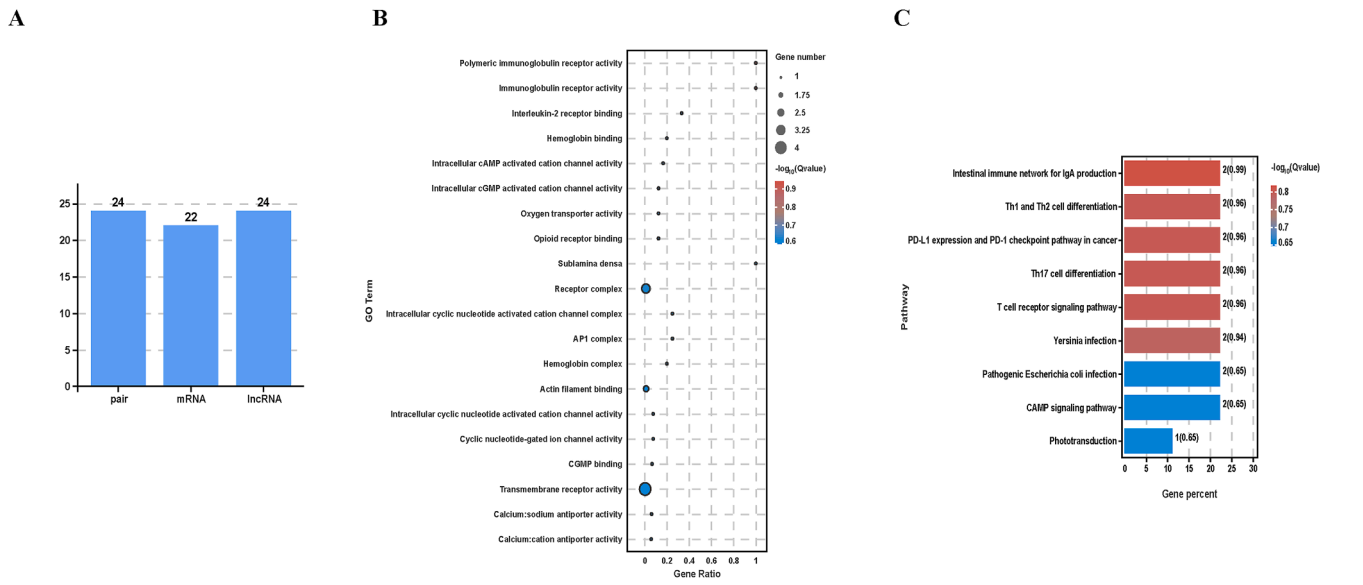

Fig. 6. GO annotation and KEGG enrichment analysis of antisense-targets of DE lncRNAs in the nesting compared to late-laying periods. A. Histogram of the number of lncRNA-mRNA antisense-target gene pairs and the corresponding number of lncRNAs and mRNAs. B. GO annotation analysis of antisense-targets of DE lncRNAs. C. KEGG enrichment analysis of antisense-targets of DE lncRNAs.

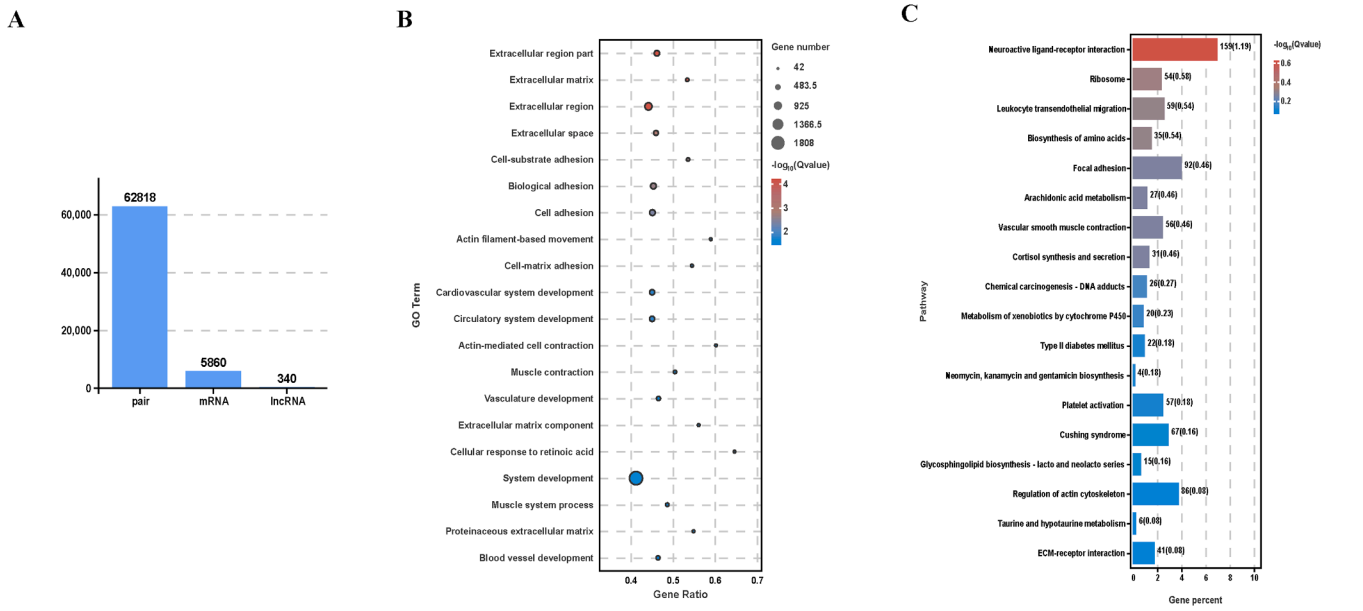

Fig. 7. GO annotation and KEGG enrichment analysis of trans-targets of DE lncRNAs in the nesting compared to late-laying periods. A. Histogram of the number of lncRNA-mRNA trans-target gene pairs and the corresponding number of lncRNAs and mRNAs. B. GO annotation analysis of trans-targets of DE lncRNAs. C. KEGG enrichment analysis of trans-targets of DE lncRNAs.

Table 5
The potential antisence-target DEGs of DE lncRNAs associated with nesting in geese.

LncRNA	Gene symbol	GO terms or pathway
MSTRG.10044.1	*v-FOS*	Reproduction and oxytocin signaling pathway
MSTRG.12265.1	*PIGR*	cell communication
MSTRG.19835.1	*HBB*	transport
MSTRG.231.1	*PDLIM1*	positive regulation of metabolic process
XR_001210447.1	*PIGR-like*	cell communication

non-invasive biomarker for cancer (Li et al. 2008). We found a significantly positive relationship between *USP36* expression and TG levels in Wanxi white geese. *HECTD3* is a ubiquitin ligase that directly binds TARA, a guanine nucleotide exchange factor involved in actin cytoskeletal reorganization, cell mobility, and cell growth (Yu et al. 2008). The gene is a miR-26a target and participates in early quail embryonic development by regulating organelle organization (Kocamis et al. 2013). *HECTD3* expression correlated positively with WBC, NEU, HCT, and PRL levels and negatively with ALP, TG, LH, E2 and P4 levels in Wanxi white geese. Gao et al. (2021) conducted a genome-wide association study to identify genetic markers associated with goose reproductive performance and egg quality traits (Gao et al. 2021). They identified 26 SNPs significantly associated with body weight at birth,

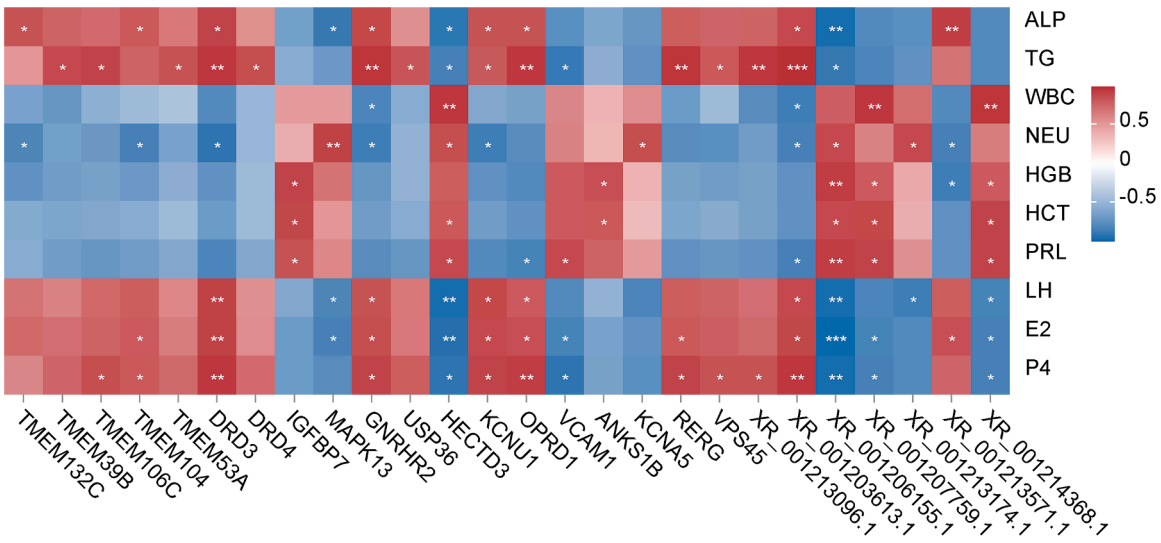

Fig. 8. Correlation analysis between phenotypic data and DEGs or DE lncRNAs. The phenotypic data comprised hematological parameters (WBC, NEU, HGB, and HCT), serum biochemicals (ALP and TG), and hormone levels (PRL, LH, E2, and P4).

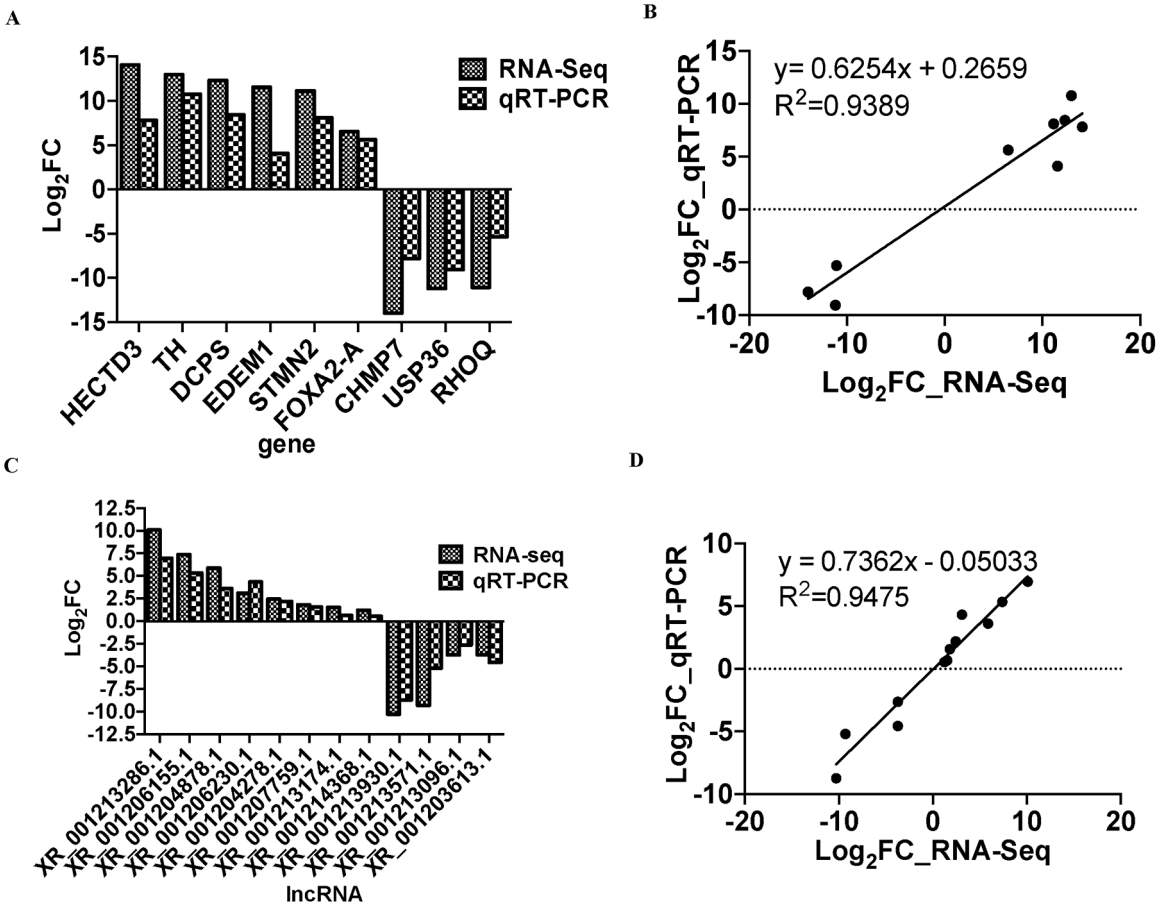

Fig. 9. Validation of randomly chosen DEGs and DE lncRNAs using qRT-PCR. The X-axis illustrates the 9 randomly selected DEGs (A) and 12 DE lncRNAs (C) for qRT-PCR, while the y-axis shows the log2 (fold change = nesting/late-laying) obtained from RNA-Seq and qRT-PCR. Different shaded bars represent the results from RNA-Seq and qRT-PCR. Regression analysis (B, D) was performed on the log2 (fold change = nesting/late-laying) values derived from RNA-Seq and qRT-PCR.

number of eggs at different ages, and egg yolk color. These findings indicated that specific genetic regions on chromosomes 35 and 5 were associated with these traits, particularly the region harboring the *TMEM161A* gene in chromosome 35. Additionally, the *TMEM132C, TMEM39B, TMEM106C, TMEM104*, and *TMEM53A* in the *TMEM* gene family were differentially expressed and a significant correlation observed between their expression and those of ALP, TG, NEU, E2, and P4 in the nesting and late-laying periods in Wanxi white geese.

The effect of dopamine on the release of hormones and neurotransmitters is associated with the D2-like receptors (*DRD2* and *DRD4*) in

birds (Neve et al. 2004). In the present study, the lncRNA MSTRG.18140.1 exhibited cis-regulatory effects on *DRD4* in the ovarian tissue of Wanxi white geese. *DRD4* has specific essential functions in avian peripheral tissues, particularly in the testes and ovaries, as the expression of this gene is downregulated in the ovarian cortex of pre-pubescent broiler breeder hens fed ad libitum from the hatching period, suggesting its potential use as a biomarker for cortical follicle development in chicken (Lv et al. 2018). *DRD3* expression was significantly higher in the pituitary of the low-density than in the high-density group of laying ducks, potentially influencing dopamine production (Liu et al. 2022a). Liu et al. (2023) demonstrated that DEGs with methylated regions were involved in neuroactive ligand-receptor interaction, calcium signaling pathway, and focal adhesion in Magang geese reared under long-light periods (Liu et al. 2023b). The present study showed that DEGs such as *OPRD1, Wnt3A, DRD3* and *DRD4* regulated these biological pathways during the nesting and the late-laying periods in Wanxi white geese. The differential expression of *OPRD1, DRD3,* and *KCNU1* was closely related with the levels of ALP, TG, LH, E2, and P4, and *OPRD1* participates in avian ovarian follicle development (Chen et al. 2021). *OPRD1* expression pattern remained consistent across various stages of oocyte maturity, from the germinal vesicle to the metaphase II stage (Böttcher et al. 2017). *KCNU1* participates in the spermatogenesis process and is differentially expressed between the testes of Landes geese and Sichuan white geese (Ran et al. 2021).

VCAM gene regulates cell adhesion and CAMs, and is differentially regulated during follicular development in Magang geese (Lei et al. 2020). There was a relationship between the expression of *VCAM* and those of TG, PRL, E2 and P4 levels during the nesting compared to the late-laying period in Wanxi white geese. Qin et al. (2021) identified 258 DEGs in Xupu goose ovarian tissues were associated with focal adhesion, ECM-receptor interaction, and N-glycan biosynthesis pathways (Qin et al. 2021). *GALNT15* was the cis-target of lncRNA XR_001203613.1, whose differential expression positively correlated with ALP, TG, LH, E2, and P4 levels in Wanxi white geese. This gene is involved in O-glycan processing. It initiates mucin-type O-glycosylation by adding N-acetylgalactosamine to serine or threonine residues, influencing processes like cell adhesion, signal transduction, molecular trafficking, and central nervous system development (Liu et al., 2022c). It also plays a role in acrosome formation, with *GALNT15* deficiency in mice shown to reduce sperm motility, causing male infertility (Takasaki et al. 2014). The *EGR1* gene regulates follicular development in Tianfu meat geese (Liu et al. 2018), and was differentially expressed in the ovaries of Wanxi white geese between the late-laying and the nesting periods. The current study showed that *COL6A3, COL6A2,* and *CHAD* were associated with focal adhesion and ECM-receptor interaction pathways, consistent with the previous findings. *COL6A3* is an extracellular matrix gene, and overexpression of *COL6A3* promotes tumor invasion and metastasis of epithelial ovarian cancer cells (Ho et al. 2024). This gene, as a cis-target of lncRNA XR_001206155.1, was negatively associated with the levels of ALP, TG, LH, E2, and P4. The *COL6A3* is a stromal extracellular matrix gene that is significantly upregulated in the theca interna of ovarian follicles, highlighting its potential involvement in the structural or functional regulation of the ovarian microenvironment (Hatzirodos et al. 2015). Furthermore, *v-Fos*, similar to *c-Fos,* and *OXTR*, were implicated in the oxytocin signaling pathway in the ovaries of Wanxi white geese. These aforementioned genes form a feedback loop that coordinates signals between the hypothalamus and pituitary gland to control gene expression in the ovaries and follicles (Liu et al. 2018).

Analysis of miRNA expression profiles in varying grades of antral follicles in Zhedong white geese revealed that the differentially expressed miRNAs were implicated in the MAPK, cytokine-receptor interactions, and Wnt signaling pathways (Yu et al. 2016a). Transcriptome analysis of pre-grade follicles of Zi geese at the peak of the menstrual cycle revealed that DEGs in grade follicle tissues were primarily associated with the PI3K-AKT and MAPK signaling pathways, which promote the development of goose grade follicles (Cao et al. 2015). In the ovaries of Wanxi white geese, *MAPK13* gene was upregulated during the nesting stage, and its expression negatively correlated with ALP, LH, and E2 levels. Previous findings indicated that *MAPK13* is upregulated in GV oocytes in adult cows and is associated with calving challenges in dairy cows (Dorji et al. 2012). *IGFBP3* is expressed in the ovaries of Sichuan white geese during the pre-laying and laying stages, and it regulates cell proliferation and differentiation (Ding et al. 2015). In the present study, the differential expression of *IGFBP7* was positively correlated with the levels of HGB, HCT and PRL in Wanxi white geese ovaries. *IGFBP7* participates in follicular development and reproduction by inhibiting estrogen synthesis in granulosa cells and inhibiting granulosa cell steroidogenesis (Tamura et al. 2007).

ANKS1B, involved in tyrosine kinase signal transduction, is primarily expressed in the brain and testis (Liu et al. 2019). Interestingly, this gene was differentially expressed in the goose ovary, and its expression positively correlated with HGB and HCT levels. Further analyses showed that the gene is a cis-target of lncRNA XR_001207759.1. Polycystic ovary syndrome suppresses *KCNA5* expression in granulosa cells, slowing down the proliferation of granulosa (Gao et al. 2020). The differential expression of this gene was positively related to NEU level, and the gene was a cis-target of XR_001213174.1 in Wanxi white geese. Monsivais et al. (2014) identified Ras-like estrogen-regulated growth factor *RERG* as an ER target by integrating ER binding data and gene expression profiles from breast cells, endometriosis, and endometrial tissues. E2 significantly increased *RERG* expression and enriched ER at the *RERG* promoter, promoting primary endometriotic cell proliferation (Monsivais et al. 2014). The present study further revealed that in Wanxi white geese, *RERG* is a cis-target of lncRNA XR_001213571.1, and its expression is closely associated with serum TG levels. *VPS45* is a member of the SM protein family involved in intracellular vesicle fusion events. The expression pattern of *VPS45* predicts the prognosis of ovarian serous cystadenocarcinoma (Yamanoi et al. 2019). In the present study, *VPS45* was further identified as a cis-target of lncRNA XR_001214368.1, and *VPS45* expression was strongly related to serum TG levels in Wanxi White geese. Inositol 1,4,5-trisphosphate receptor type 3 (*ITPR3*) regulates the GnRH signaling and the calcium signaling, and its expression is significantly different between broody and egg-laying Zhedong white geese (Yu et al. 2016b). Mammalian type 2 GnRHR specifically responds to GnRH2 by producing inositol phosphate, LH, and FSH (Millar et al. 2001). The XR_001213096.1-*ITPR3* and MSTRG.19948.1-*GnRHR2* exhibited cis-regulation in Wanxi white geese. Furthermore, XR_001213096.1 was positively linked to TG and P4 levels, and *GnRHR2* was positively associated with ALP, TG, LH, E2, and P4 levels. These results indicated that the cis-regulation affects nesting in geese by regulating follicular development.

Conclusions

In summary, in this study, the difference in hematopoietic parameters, serum hormones, histomorphometry, and gene expression in Wanxi white geese between late-laying and nesting periods was explored. Molecular profiling uncovered cis-regulation of DEGs and DE lncRNAs in the ovaries of Wanxi white geese involved with geese nesting. Functional enrichment analysis revealed that various signaling pathways, including focal adhesion and ECM-receptor, are involved in the nesting occurrence. Several specific DEGs and DE lncRNAs were closely related to the levels of blood indexes, which indicated that they might be associated with nesting and affect geese reproduction. These findings indicate that the DEGs, DE lncRNAs, and related signaling pathways significantly impact the differences observed between nesting and late-laying ovaries. The findings of the present study deepen the understanding of ovarian physiology in Wanxi white geese, offering valuable insights into avian reproductive health.

Declaration of generative AI and AI-assisted technologies in the writing process

During the preparation of this work, the author(s) only used these technologies to improve readability and language.

Declaration of interests

The authors declare that they have no known competing financial interests or personal relationships that could have appeared to influence the work reported in this paper.

Acknowledgments

The work was supported in part by the the University Research Project of Anhui Province (no. 2023AH051872, KJ2020A0081), Anhui Province Young Top Talents Project (no. WJMR2023132), Anhui Province Science and Technology Major Project (no. 17030701004), National Natural Science Foundation of China (no. 32002160), Local Goose Gene Bank in Anhui Province, the Program of Anhui Provincial Key Laboratory of Livestock and Poultry Product Safety Engineering (no. XM2403), the Anhui Province Key Research and Development Program Project (no. 202204c06020074), Veterinary Science Peak Discipline Project of Anhui Science and Technology University (no. XK-XJGF002), the Foundation of Anhui Science and Technology University (no. DKYJ201901), the Graduate Program of the Anhui Provincial Department of Education (no. 2023cxcysj175).

Supplementary materials

Supplementary material associated with this article can be found, in the online version, at doi:10.1016/j.psj.2025.104764.

Data availability

The transcriptome sequencing data were deposited in the Sequence Read Archive (SRA) database (https://www.ncbi.nlm.nih.gov/sra) of NCBI under the BioProject accession numbers PRJNA1161360 and SAMN43775953 to 43775958, and the SRA project accession numbers SRR 30688733 to 30688738.

References

Alvarenga, R.R., Zangeronimo, M.G., Pereira, L.J., Rodrigues, P.B., Gomide, E.M., 2011. Lipoprotein metabolism in poultry. World. Poult. Sci. J. 67, 431–440.
Arroba, A.I., Frago, L.M., Argente, J., Chowen, J.A., 2005. Oestrogen requires the insulin-like growth factor-I receptor for stimulation of prolactin synthesis via mitogen-activated protein kinase. J. Neuroendocrinol. 17, 97–104.
Bao, Q., Gu, W., Song, L., Weng, K., Cao, Z., Zhang, Y., Zhang, Y., Ji, T., Xu, Q., Chen, G., 2023. The photoperiod-driven cyclical secretion of pineal melatonin regulates seasonal reproduction in geese (Anser cygnoides). Int. J. Mol. Sci. 24, 11998.
Bao, Q., Zhang, Y., Yao, Y., Luo, X., Zhao, W., Wang, J., Chen, G., Xu, Q., 2022. Characteristics of the mating behavior of domesticated geese from Anser cygnoides and Anser anser. Anim. (Basel) 12, 2326.
Böttcher, B., Seeber, B., Leyendecker, G., Wildt, L., 2017. Impact of the opioid system on the reproductive axis. Fertil. Steril. 108, 207–213.
Cao, R., Wu, W.J., Zhou, X.L., Xiao, P., Wang, Y., Liu, H.L., 2015. Expression and preliminary functional profiling of the let-7 family during porcine ovary follicle atresia. Mol. Cell. 38, 304–311.
Chen, X., Liu, X., Du, Y., Wang, B., Zhao, N., Geng, Z., 2018. Green forage and fattening duration differentially modulate cecal microbiome of Wanxi white geese. PLoS One 13, e0204210.
Chen, X., Sun, X., Chimbaka, I.M., Qin, N., Xu, X., Liswaniso, S., Xu, R., Gonzalez, J.M., 2021. Transcriptome analysis of ovarian follicles reveals potential pivotal genes associated with increased and decreased rates of chicken egg production. Front. Genet. 12, 622751.
Ding, N., Han, Q., Zhao, X.Z., Li, Q., Li, J., Zhang, H.F., Gao, G.L., Luo, Y., Xie, Y.H., Su, J., Wang, Q.G., 2015. Differential gene expression in pre-laying and laying period ovaries of Sichuan White geese (Anser cygnoides). Genet. Mol. Res. 14, 6773–6785.
Djermanovic, V., Milojevic, M., Bozickovic, I., 2024. Possibilities of productive and reproductive performance improvement in geese: part II non-genetic factors. World. Poult. Sci. J. 80, 403–422.
Dorji, Y.Ohkubo, Miyoshi, K., Yoshida, M., 2012. Gene expression differences in oocytes derived from adult and prepubertal Japanese black cattle during in vitro maturation. Reprod. Domest. Anim. 47, 392–402.
Fraile, J.M., Campos-Iglesias, D., Rodriguez, F., Astudillo, A., Vilarrasa-Blasi, R., Verdaguer-Dot, N., Prado, M.A., Paulo, J.A., Gygi, S.P., Martin-Subero, J.I., Freije, J. M.P., Lopez-Otin, C., 2018. Loss of the deubiquitinase USP36 destabilizes the RNA helicase DHX33 and causes preimplantation lethality in mice. J. Biol. Chem. 293, 2183–2194.
Gao, G., Gao, D., Zhao, X., Xu, S., Zhang, K., Wu, R., Yin, C., Li, J., Xie, Y., Hu, S., Wang, Q., 2021. Genome-wide association study-based identification of SNPs and haplotypes associated with goose reproductive performance and egg quality. Front. Genet. 12, 602583.
Gao, L., Wu, D., Wu, Y., Yang, Z., Sheng, J., Lin, X., Huang, H., 2020. MiR-3940-5p promotes granulosa cell proliferation through targeting KCNA5 in polycystic ovarian syndrome. Biochem. Bioph. Res. Co. 524, 791–797.
Hatzirodos, N., Hummitzsch, K., Irving-Rodgers, H.F., Rodgers, R.J., 2015. Transcriptome comparisons identify new cell markers for theca interna and granulosa cells from small and large antral ovarian follicles. PLoS One 10, e0119800.
Ho, C.M., Yen, T.L., Chang, T.H., Huang, S.H., 2024. COL6A3 exosomes promote tumor dissemination and metastasis in epithelial ovarian cancer. Int. J. Mol. Sci. 25, 8121.
Kocamis, H., Hossain, M.M., Cinar, M.U., Salilew-Wondim, D., Mohammadi-Sangcheshmeh, A., Tesfaye, D., Hölker, M., Schellander, K., 2013. Expression of microRNA and microRNA processing machinery genes during early quail (Coturnix japonica) embryo development. Poult. Sci. 92, 787–797.
Lei, M., Chen, R., Qin, Q., Zhu, H., Shi, Z., 2020. Transcriptome analysis to unravel the gene expression profile of ovarian follicular development in Magang goose. J. Reprod. Dev. 66, 331–340.
Li, J., Olson, L.M., Zhang, Z., Li, L., Bidder, M., Nguyen, L., Pfeifer, J., Rader, J.S., 2008. Differential display identifies overexpression of the USP36 gene, encoding a deubiquitinating enzyme, in ovarian cancer. Int. J. Med. Sci. 5, 133–142.
Liu, P.H., Chuang, G.T., Hsiung, C.N., Yang, W.S., Ku, H.C., Lin, Y.C., Chen, Y.S., Huang, Y.Y., Lin, C.H., Li, W.Y., Lin, J.W., Hsu, C.N., Hwang, J.J., Liao, K.C., Hsieh, M.L., Lee, H.L., Shen, C.Y., Chang, Y.C., 2022c. A genome-wide association study for melatonin secretion. Sci. Rep. 12, 8025.
Liu, G., Guo, Z., Zhao, X., Sun, J., Yue, S., Li, M., Chen, Z., Ma, Z., Zhao, H., 2023a. Whole genome resequencing identifies single-nucleotide polymorphism markers of growth and reproduction traits in Zhedong and Zi crossbred geese. Gene. (Basel) 14, 487.
Liu, H., Wang, J., Li, L., Han, C., He, H., Xu, H., 2018. Transcriptome analysis revealed the possible regulatory pathways initiating female geese broodiness within the hypothalamic-pituitary-gonadal axis. PLoS One 13, e0191213.
Liu, H., Xiong, X., Pu, F., Wang, J., Li, Y., Xi, Y., Ma, S., Bai, L., Zhang, R., Liang, L., Yang, C., 2022a. Stocking density affects transcriptome changes in the hypothalamic-pituitary-gonadal axis and reproductive performance in ducks. Ital. J. Anim. Sci. 21, 955–966.
Liu, J., Xu, Y., Wang, Y., Zhang, J., Fu, Y., Liufu, S., Jiang, D., Pan, J., Ouyang, H., Huang, Y., Tian, Y., Shen, X., 2023b. The DNA methylation status of the serotonin metabolic pathway associated with reproductive inactivation induced by long-light exposure in Magang geese. BMC Genomics 24, 355.
Liu, J., Zhang, D., Zhang, Z., Chai, W., Zhang, J., Li, M., Wang, Y., Zhang, S., Zhu, M., 2022b. Comparison of body size and reproductive hormones in high- and low-yielding Wulong geese. Poult. Sci. 101, 101618.
Liu, R., Chen, Z., Wang, S., Zhao, G., Gu, Y., Han, Q., Chen, B., 2019. Screening of key genes associated with R-CHOP immunochemotherapy and construction of a prognostic risk model in diffuse large B-cell lymphoma. Mol. Med. Rep. 20, 3679–3690.
Lv, C., Mo, C., Liu, H., Wu, C., Li, Z., Li, J., Wang, Y., 2018. Dopamine D2-like receptors (DRD2 and DRD4) in chickens: tissue distribution, functional analysis, and their involvement in dopamine inhibition of pituitary prolactin expression. Gene 651, 33–43.
Millar, R., Lowe, S., Conklin, D., Pawson, A., Maudsley, S., Troskie, B., Ott, T., Millar, M., Lincoln, G., Sellar, R., Faurholm, B., Scobie, G., Kuestner, R., Terasawa, E., Katz, A., 2001. A novel mammalian receptor for the evolutionarily conserved type II GnRH. P. Natl. Acad. Sci. USA 98, 9636–9641.
Monsivais, D., Dyson, M.T., Yin, P., Coon, J.S., Navarro, A., Feng, G., Malpani, S.S., Ono, M., Ercan, C.M., Wei, J.J., Pavone, M.E., Su, E., Bulun, S.E., 2014. ERβ- and prostaglandin E2-regulated pathways integrate cell proliferation via ras-like and estrogen-regulated growth inhibitor in endometriosis. Mol. Endocrinol. 28, 1304–1315.
Neve, K.A., Seamans, J.K., Trantham-Davidson, H., 2004. Dopamine receptor signaling. J. Recept. Signal Transduct. Res. 24, 165–205.
Palo, P.E., Sell, J.L., Piquer, F.J., Vilaseca, L., Soto-Salanova, M.F., 1995. Effect of early nutrient restriction on broiler chickens. 2. Performance and digestive enzyme activities. Poult. Sci. 74, 1470–1483.
Qin, H., Li, X., Wang, J., Sun, G., Mu, X., Ji, R., 2021. Ovarian transcriptome profile from pre-laying period to broody period of Xupu goose. Poult. Sci. 100, 101403.
Ran, J.S., Yin, L.Q., Li, J.J., Tang, Y.Q., Huang, J., Ren, P., Zhang, X.X., Li, S.M., Liu, Y.P., 2022. Integrated analysis of microRNA and mRNA interactions in ovary of counter-season breeding and egg-ceased geese (Anser cygnoides). Theriogenology 186, 146–154.
Ran, M., Huang, H., Hu, B., Hu, S., Hu, J., Li, L., He, H., Liu, H., Wang, J., 2021. Comparative analysis of testicular histology and lncRNA-mRNA expression patterns between Landes geese (Anser anser) and Sichuan white geese (Anser cygnoides). Front. Genet. 12, 627384.
Soriano, G.A.M., de Ruediger, F.R., Zundt, M., Gomes, M., de Souza, L.F.A., Giometti, I. C., de Paula Nogueira, G., Zanelli, G.R., de Almeida Rego, F.C., Castilho, C., 2018.

Characterization of the LH peak after short and long fixed-time artificial insemination protocols in sheep raised in the tropics. Anim. Sci. J. 89, 1245–1252.
Takasaki, N., Tachibana, K., Ogasawara, S., Matsuzaki, H., Hagiuda, J., Ishikawa, H., Mochida, K., Inoue, K., Ogonuki, N., Ogura, A., Noce, T., Ito, C., Toshimori, K., Narimatsu, H., 2014. A heterozygous mutation of GALNTL5 affects male infertility with impairment of sperm motility. P. Natl. Acad. Sci. USA 111, 1120–1125.
Tamura, K., Matsushita, M., Endo, A., Kutsukake, M., Kogo, H., 2007. Effect of insulin-like growth factor-binding protein 7 on steroidogenesis in granulosa cells derived from equine chorionic gonadotropin-primed immature rat ovaries. Biol. Reprod. 77, 485–491.
Wang, Z., Lu, L., Gu, T., Hou, L., Du, L., Zhang, Y., Zhang, Y., Xu, Q., Chen, G., 2021a. The effects of FAR1 and TGFBRAP1 on the proliferation and apoptosis of follicular granulosa cells in goose (Anser cygnoides). Gene 769, 145194.
Wang, Z., Wang, L., Zhang, Y., Yao, Y., Zhao, W., Xu, Q., Chen, G., 2021b. Characterization of ovarian morphology and reproductive hormones in Zhedong white geese (Anser cygnoides domesticus) during the reproductive cycle. J. Anim. Physiol. Anim. Nutr. (Berl) 105, 938–945.
Yamanoi, K., Baba, T., Abiko, K., Hamanishi, J., Yamaguchi, K., Murakami, R., Taki, M., Hosoe, Y., Murphy, S.K., Konishi, I., Mandai, M., Matsumura, N., 2019. Acquisition of a side population fraction augments malignant phenotype in ovarian cancer. Sci. Rep. 9, 14215.
Yu, J., He, K., Ren, T., Lou, Y., Zhao, A., 2016a. High-throughput sequencing reveals differential expression of miRNAs in prehierarchal follicles of laying and brooding geese. Physiol. Genom. 48, 455–463.
Yu, J., Lan, J., Zhu, Y., Li, X., Lai, X., Xue, Y., Jin, C., Huang, H., 2008. The E3 ubiquitin ligase HECTD3 regulates ubiquitination and degradation of Tara. Biochem. Bioph. Res. Co. 367, 805–812.
Yu, J., Lou, Y., Zhao, A., 2016b. Transcriptome analysis of follicles reveals the importance of autophagy and hormones in regulating broodiness of Zhedong white goose. Sci. Rep. 6, 36877.
Zhao, W., Yuan, T., Fu, Y., Niu, D., Chen, W., Chen, L., Lu, L., 2021. Seasonal differences in the transcriptome profile of the Zhedong white goose (Anser cygnoides) pituitary gland. Poult. Sci. 100, 1154–1166.